

# Theory of dielectrophoresis in colloidal suspensions

L. Dong,<sup>a)</sup> J. P. Huang,<sup>b)</sup> and K. W. Yu<sup>c)</sup>

*Department of Physics, The Chinese University of Hong Kong, Shatin, New Territories, Hong Kong*

(Received 21 April 2003; accepted 15 March 2004)

A theoretical study of the dielectrophoretic (DEP) spectrum of a pair of touching colloidal particles or biological cells in a host fluid under the application of a nonuniform alternating current (ac) electric field is presented. The main objective of this work is to investigate the correlation effects due to the presence of mutual polarization on the DEP spectrum. In particular, we employ the multiple image method to account for the effect of multiple images, and obtain an analytic expression for the DEP force. It is found that, at low frequencies, the DEP force can be enhanced (reduced) significantly for the longitudinal (transverse) field case due to the presence of multiple images. The numerical results can be well understood in the spectral representation theory. To first order in the dipole interaction, our results reduce to the established formula derived by an alternative method. Our approach demonstrates the importance of the correlation effects in ac electrokinetic phenomena of colloidal suspensions. © 2004 American Institute of Physics.

[DOI: 10.1063/1.1737050]

## I. INTRODUCTION

Dielectrophoresis describes the translational motion of colloidal particles or biological cells caused by the interaction between the induced dipole moment and the external nonuniform electric field.<sup>1</sup> The force acting on the particle is known as the dielectrophoretic (DEP) force ( $F_{\text{DEP}}$ ), and is dependent on the frequency of the external ac electric field,<sup>1</sup> as well as on the magnitude of the complex dielectric constant (permittivity and conductivity) of the particles relative to that of the medium. The frequency at which the DEP force vanishes is the crossover frequency ( $f_{\text{CF}}$ ). The analysis of  $f_{\text{CF}}$  against the medium conductivity can be used to investigate the dielectric properties of colloidal particles.<sup>2-4</sup> While dielectrophoresis is typically used for manipulation and separation of micrometer-size ( $\sim \mu\text{m}$ ) particles such as biological cells, it has recently been successfully applied to submicron-size particles as well. Specific applications include diverse problems in medicine, colloidal science, and nanotechnology.<sup>2,3,5-9</sup>

In the dilute limit, one can focus on the DEP spectrum of an individual particle, by ignoring the mutual interactions between the particles. However, if the suspension is not dilute, the situation is complicated by the mutual interactions between the particles. In addition, the particles may aggregate due to the presence of an external field, even when the suspension is initially in the dilute limit. In this case, the mutual interactions are expected to play a role.

In this work, we investigate further the DEP spectrum of two approaching spherical colloidal particles under a nonuniform ac electric field. It is known that the Maxwell-Wagner

interfacial polarization can be influenced by the mutual interaction between approaching particles.<sup>10</sup> We will use the multiple image method<sup>11</sup> to account for the effect of multiple images.

Recently, in Ref. 12, the multiple image method has been demonstrated to be in agreement with a multipole expansion method.<sup>13</sup> Based on the multipole expansion method, the potentials are expanded inside and outside the particles in terms of solid spherical harmonics, and the multipole moments are then obtained by solving a set of linear equations determined by the appropriate boundary conditions. As stated in Ref. 12, this multipole expansion theory and our multiple image method are based on different pictures and there exists no direct and exact equivalent relationship between them. The calculation of the interparticle energy using the multiple image method and the multipole expansion method shows that the multiple image method reflects, although not exactly, some characteristics of the third order multipole expansion method, i.e., an octupole effect.

In this work, by employing the spectral representation theory,<sup>14</sup> we will derive an analytic expression for the DEP force and hence determine the DEP spectrum as well as crossover frequency.

In Ref. 4, we investigated in detail the DEP crossover frequency of charged colloidal suspensions, with a focus on the charging effect. In this paper we aim to investigate the DEP spectra of uncharged colloidal suspensions. We would investigate two cases: (1) longitudinal field case where the applied field is parallel to the line joining the centers of the two particles, and (2) transverse field case where the applied field is perpendicular to the line joining the centers of the two particles.

This paper is organized as follows. In Sec. II, we present the formalism based on the multiple image method, which is followed by the derivations of the analytic expression for the DEP force in the spectral representation theory. In Sec. III, we numerically investigate the DEP spectrum under various

<sup>a)</sup>Present address: Biophysics and Statistical Mechanics Group, Laboratory for Computational Engineering, Helsinki University of Technology, P.O. Box 9203, FIN-02015 HUT, Finland.

<sup>b)</sup>Present address: Max Planck Institute for Polymer Research, Ackermannweg 10, 55128 Mainz, Germany.

<sup>c)</sup>Electronic mail: kwyu@phy.cuhk.edu.hk

conditions. The discussion and conclusion is given in Sec. IV.

## II. FORMALISM

### A. Multiple image method for a pair of colloidal particles

Consider an isolated spherical colloidal particle or biological cell with diameter  $D$ , of complex dielectric constant  $\tilde{\epsilon}_1 = \epsilon_1 + \sigma_1/(i2\pi f)$  dispersed in a host medium of  $\tilde{\epsilon}_2 = \epsilon_2 + \sigma_2/(i2\pi f)$ , where  $\epsilon$  and  $\sigma$  denote the real dielectric constant and conductivity, respectively,  $f$  stands for the frequency of the external electric field, and  $i \equiv \sqrt{-1}$ . In the presence of a nonuniform electric field  $\mathbf{E}$ , the particle experiences a DEP force.<sup>15</sup>

$$\mathbf{F}_{\text{DEP}} = \frac{1}{4}\pi\epsilon_2 D^3 \text{Re}[\tilde{b}] \nabla |\mathbf{E}|^2, \quad (1)$$

where  $\tilde{b} = (\tilde{\epsilon}_1 - \tilde{\epsilon}_2)/(\tilde{\epsilon}_1 + 2\tilde{\epsilon}_2)$  is the dipole factor of the isolated particle, and  $\text{Re}[\dots]$  means the real part of  $[\dots]$ . In particular, the frequency at which  $\mathbf{F}_{\text{DEP}} = 0$  is just the crossover frequency ( $f_{\text{CP}}$ ). The relation between the dipole factor  $\tilde{b}$  and the dipole moment  $\tilde{p}$  of an isolated particle has the form

$$\tilde{p} = \frac{1}{8}\pi\epsilon_2 D^3 \tilde{b} \mathbf{E}. \quad (2)$$

Note that the real part  $\epsilon_2$  should be used to compute the complex dipole moment.

When the particles approach and get close to each other, the effect of multiple images becomes significant in the DEP force, and thus should be taken into account.<sup>16</sup> Let us consider a pair of touching spherical particles with center-to-center separation  $R$  suspended in a medium. In this case, the dipole moment of a pair is given by<sup>11</sup>

$$\tilde{p}^* = \tilde{p} \sum_{n=0}^{\infty} (Y\tilde{b})^n \left( \frac{\sinh \alpha}{\sinh(n+1)\alpha} \right)^3, \quad (3)$$

where  $\alpha$  satisfies  $\cosh \alpha = R/D$ , and the polarization index  $Y=2$  (or  $-1$ ) for the longitudinal (or transverse) field case. In view of the relation between the dipole moment and the dipole factor, we can obtain the dipole factor of a pair:

$$\tilde{b}^* = \tilde{b} \sum_{n=0}^{\infty} (Y\tilde{b})^n \left( \frac{\sinh \alpha}{\sinh(n+1)\alpha} \right)^3. \quad (4)$$

We should remark that this equation includes the effect of multiple images. When the summation is taken up to 1, this equation represents the first-order dipole-induced-dipole interaction, i.e., the interaction between the dipole induced by the other dipole (namely, the maximum number of images under consideration is one. Accordingly, this dipole factor is given by

$$\begin{aligned} \tilde{b}^*(1) &= \tilde{b} \sum_{n=0}^1 (Y\tilde{b})^n \left( \frac{\sinh \alpha}{\sinh(n+1)\alpha} \right)^3 \\ &= \tilde{b} \left[ 1 + (Y\tilde{b}) \left( \frac{D}{2R} \right)^3 \right], \end{aligned} \quad (5)$$

namely,

$$\tilde{b}_L^*(1) = \tilde{b} \left[ 1 + (2\tilde{b}) \left( \frac{D}{2R} \right)^3 \right] = \tilde{b} \frac{1 - (\tilde{b}^2/16)(D/R)^6}{1 - (\tilde{b}/4)(D/R)^3}, \quad (6)$$

$$\tilde{b}_T^*(1) = \tilde{b} \left[ 1 - \tilde{b} \left( \frac{D}{2R} \right)^3 \right] = \tilde{b} \frac{1 - (\tilde{b}^2/64)(D/R)^6}{1 + (\tilde{b}/8)(D/R)^3}, \quad (7)$$

respectively, for the longitudinal field ( $L$ ) and transverse field ( $T$ ) cases. When  $|\tilde{b}| < 1$  and  $D/R \approx 1$  (for two touching particles herein), we can rewrite  $\tilde{b}_L^*(1)$  and  $\tilde{b}_T^*(1)$  as

$$\tilde{b}_L^* = \frac{\tilde{b}}{1 - \tilde{b}/4}, \quad (8)$$

$$\tilde{b}_T^* = \frac{\tilde{b}}{1 + \tilde{b}/8}. \quad (9)$$

These results coincide with those predicted by Jones<sup>17</sup> where a field method is performed. By using this field model, Jones took into account the effect of the first-order dipole-induced-dipole interaction on the local field inside the particles.

### B. Spectral representation and dispersion spectrum

In a recent paper,<sup>18</sup> we studied the dielectric behavior of colloidal suspensions by employing the Bergman-Milton spectral representation of the effective dielectric constant.<sup>14</sup> The spectral representation is a rigorous mathematical formalism of the effective dielectric constant of a composite material. By means of the spectral representation, we derived the dielectric dispersion spectrum in terms of the electrical and structure parameters of the particles. The essence of the spectral representation is to define the following transformations. If we denote a complex material parameter

$$\tilde{s} = \left( 1 - \frac{\tilde{\epsilon}_1}{\tilde{\epsilon}_2} \right)^{-1}, \quad (10)$$

then the dipole factor  $\tilde{b}^*$  admits the general form

$$\tilde{b}^* = \sum_m \frac{F^{(m)}}{\tilde{s} - s^{(m)}}, \quad (11)$$

where  $m$  is a positive integer, i.e.,  $m=1,2,\dots$ , and  $F^{(m)}$  and  $s^{(m)}$  are the  $m$ th microstructure parameters of the composite material.<sup>14</sup>

Thus the spectral representation offers the advantage of the separation of material parameters (namely, the dielectric constant and conductivity) from the particle structure parameters (i.e., the size of colloids, the separation between colloids, and the particle alignment against the direction of the external field, like transverse field or longitudinal field cases), thus simplifying the study. Using the spectral representation, one can readily derive the dielectric dispersion spectrum, i.e., the dispersion strength as well as the characteristic frequency are explicitly expressed in terms of the structure parameters and the material parameters.<sup>18</sup> The actual frequency dependence of the real and imaginary parts of the dielectric constant in the relaxation region can be uniquely determined by the Debye relaxation spectrum, parametrized by the characteristic frequencies and the dispersion strengths. So, we can study the impact of these param-

eters on the dispersion spectrum directly. In what follows, we further express the dipole factor  $\tilde{b}$  and  $\tilde{b}^*$  in the spectral representation. The dipole factor  $\tilde{b}$  admits the form  $\tilde{b} = F^{(1)}/(\tilde{s} - s^{(1)})$ , where  $F^{(1)} = -1/3$  and  $s^{(1)} = 1/3$ . To make this approach tractable, we further define a dielectric-constant contrast and a conductivity contrast, respectively,<sup>18</sup>

$$s = (1 - \epsilon_1/\epsilon_2)^{-1} \quad \text{and} \quad t = (1 - \sigma_1/\sigma_2)^{-1}. \quad (12)$$

After simple manipulations, the dipole factor of an isolated particle becomes<sup>16</sup>

$$\tilde{b} = \frac{F^{(1)}}{s - s^{(1)}} + \frac{\delta\epsilon^{(1)}}{1 + if/f_c^{(1)}}, \quad (13)$$

where  $f_c^{(1)}$  is the characteristic frequency, and  $\delta\epsilon^{(1)}$  is the dispersion magnitude:

$$\delta\epsilon^{(1)} = F^{(1)} \frac{s - t}{(t - s^{(1)})(s - s^{(1)})}, \quad (14)$$

$$f_c^{(1)} = \frac{1}{2\pi} \frac{\sigma_2}{\epsilon_2} \frac{s(t - s^{(1)})}{t(s - s^{(1)})}. \quad (15)$$

Similarly,  $\tilde{b}^*$  can be exactly rewritten in the spectral representation as<sup>16</sup>

$$\tilde{b}^* = \sum_{m=1}^{\infty} \frac{F^{(m)}}{\tilde{s} - s^{(m)}}, \quad (16)$$

where

$$F^{(m)} = -\frac{4}{3}m(m+1)\sinh^3 \alpha e^{-(2m+1)\alpha},$$

$$s^{(m)} = \frac{1}{3}[1 - Y e^{-(1+2m)\alpha}]. \quad (17)$$

It is worth noting that  $F_L^{(m)} = F_T^{(m)}$ . In fact, for the longitudinal field and transverse field cases,  $F_L^{(m)}$  is naturally equal to  $F_T^{(m)}$ . Both of them should satisfy a sum rule predicted by the spectral representation theory for two identical particles, that is,

$$\sum_{m=1}^{\infty} F_L^{(m)} = -\frac{1}{3} = \sum_{m=1}^{\infty} F_T^{(m)}.$$

In the above derivation, we have used the identity

$$\frac{1}{\sinh^3 x} = \sum_{m=1}^{\infty} 4m(m+1)e^{-(1+2m)x}. \quad (18)$$

Thus, the spectral representation of  $\tilde{b}^*$  consists of a discrete set of simple poles.<sup>16</sup> The  $m=1$  pole  $s^{(1)}$  deviates significantly from 1/3 while  $s^{(1)}$  becomes smaller than 1/3 in the touching limit ( $\alpha \rightarrow 0$ ). Next, we will show that this pole gives a significant contribution to the DEP spectrum at low frequencies. As  $m$  increases, however, the series  $s^{(m)}$  converges to 1/3, giving rise to a dominant contribution near the isolated-sphere characteristic frequency. Moreover, each term in the spectral representation expression of  $\tilde{b}^*$  can be rewritten as

$$\frac{F^{(m)}}{\tilde{s} - s^{(m)}} = \frac{F^{(m)}}{s - s^{(m)}} + \frac{\delta\epsilon^{(m)}}{1 + if/f_c^{(m)}}, \quad (19)$$

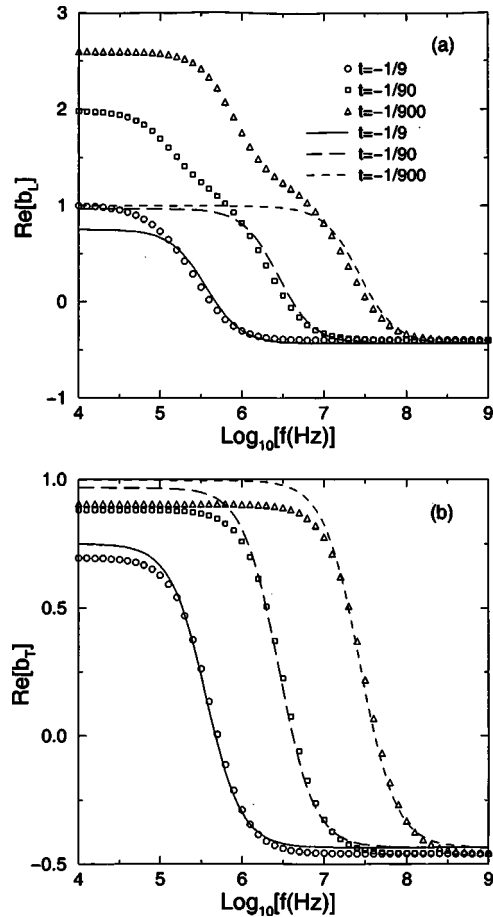


FIG. 1. The DEP spectrum (real part of the dipole factor) for an isolated sphere (lines) and touching spheres (symbols) for three different conductivity contrasts  $t$  for (a) the longitudinal field and (b) transverse field cases, respectively. Parameters:  $s = 1.1$  and  $\sigma_2 = 2.8 \times 10^{-4}$  S/m.

where  $\delta\epsilon^{(m)}$  and  $f_c^{(m)}$  are the dispersion magnitudes and the characteristic frequencies, obtained, respectively, by replacing  $F^{(1)}$  and  $s^{(1)}$  in the expressions of  $\delta\epsilon^{(1)}$  and  $f_c^{(1)}$  in Eqs. (14) and (15) with  $F^{(m)}$  and  $s^{(m)}$ . Note that the first ( $m=1$ ) characteristic frequency of a pair is significantly lower than that of an isolated particle in the longitudinal field case. Obviously, in this case the real part of  $\tilde{b}^*$  can be expressed as

$$\text{Re}[\tilde{b}^*] = \sum_{m=1}^{\infty} \left( \frac{F^{(m)}}{s - s^{(m)}} + \frac{\delta\epsilon^{(m)}}{1 + (f/f_c^{(m)})^2} \right). \quad (20)$$

It is worth remarking that Eq. (20) is indeed the exact transformation of Eq. (4), which represents the infinite-order dipole-induced-dipole interaction. Thus, we have the DEP force

$$F_{\text{DEP}}^* = \frac{1}{4}\pi\epsilon_2 D^3 \text{Re}[\tilde{b}^*] |\nabla|\mathbf{E}|^2 \quad (21)$$

in terms of a series of dispersion strengths ( $\delta\epsilon^{(m)}$ ) and characteristic frequencies ( $f_c^{(m)}$ ). Hence, the DEP spectrum of two touching spheres consists of a series of subdispersions. In the next section we will investigate the effect of multiple images on the DEP spectrum of a pair of touching particles.

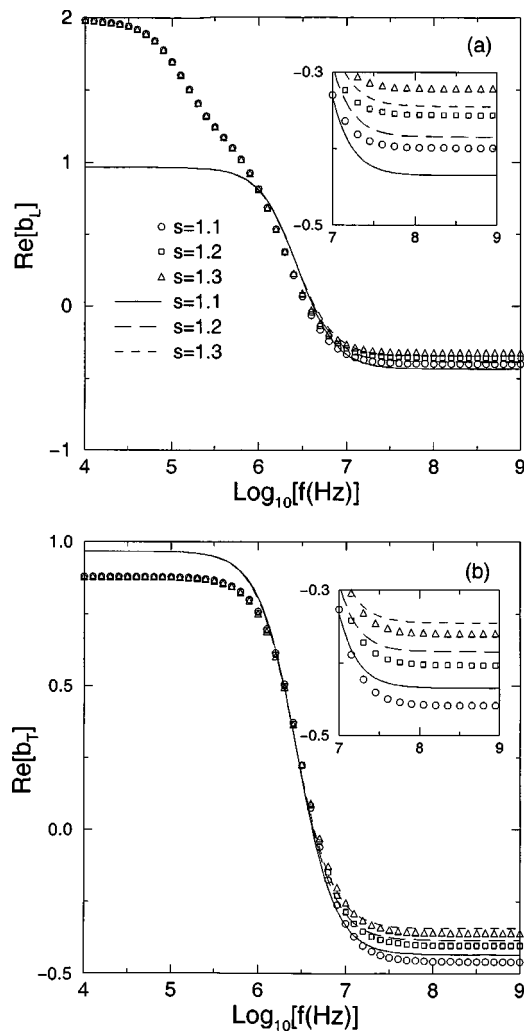


FIG. 2. Similar to Fig. 1 but for three different dielectric contrasts  $s$ . Insets: Enlargement of the high frequency spectrum for clarity. Parameters:  $t = -1/90$  and  $\sigma_2 = 2.8 \times 10^{-4}$  S/m.

### III. NUMERICAL RESULTS

We are now in a position to investigate the DEP spectrum numerically, based on Eq. (4) and Eq. (20). Please note Eq. (20) is an exact transformation of Eq. (4), as stated above. To discuss the effect of the images (Figs. 5 and 6), we resort to Eq. (20). Moreover, it is worth noting that both Eq. (4) and Eq. (20) are convergent for the parameters in use (Fig. 6). Hence, for our numerical calculations it suffices to set the upper limit of  $m$  to be 100. We should remark that, we selected the large variation of  $t$  because the variation of conductivities of colloidal particles (e.g., biological cells) can be very large, whereas we selected small variation of  $s$  because the variation of real dielectric constants of various colloidal particles is small indeed.

Figure 1 shows the effect of conductivity contrasts ( $t$ ) on the DEP spectrum for isolated particles and touching particles for (a) the longitudinal field case and (b) the transverse field case, respectively. Here the DEP spectrum is denoted by the real part of the dipole factor. From Fig. 1, it is shown that the effect of multiple images plays an important role in the DEP spectrum in the low frequency region. The effect of

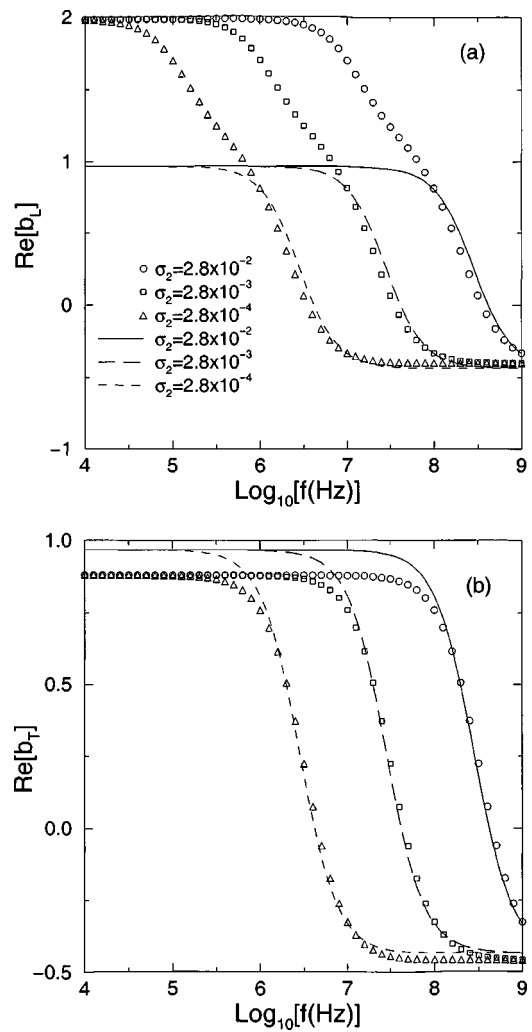


FIG. 3. Similar to Fig. 1 but for three different medium conductivities  $\sigma_2$ . Parameters:  $s = 1.1$  and  $t = -1/90$ .

multiple images increases (decreases) the induced-dipole moment of the individual particles in the longitudinal (transverse) geometry, and hence the DEP force can be enhanced (reduced) significantly for the longitudinal (transverse) field case. In particular, a subdispersion, which is located at the low frequency region, appears for the longitudinal field case [Fig. 1(a)] but not for the transverse field case [Fig. 1(b)], due to the highly anisotropic presence of multiple images. Moreover, for both the longitudinal field and transverse field cases, decreasing the conductivity contrast  $t$  leads to the dispersions being located at lower frequencies (redshifted), together with a lower DEP force within the corresponding frequency region.

Some interesting results are found for the crossover frequency in which the DEP force changes its sign. It is shown that the crossover frequency for the longitudinal (transverse) field case  $f_{CF}^L$  ( $f_{CF}^T$ ) will move to lower frequencies (higher frequencies) in touching case than in isolated case, which is caused by the effect of multiple images. In addition, for a smaller  $t$ , we observe a smaller  $f_{CF}^L$  or  $f_{CF}^T$ .

In Fig. 2, we investigate the effect of the dielectric contrast ( $s$ ) on the DEP spectrum for (a) the longitudinal field case and (b) the transverse field case, respectively. We se-

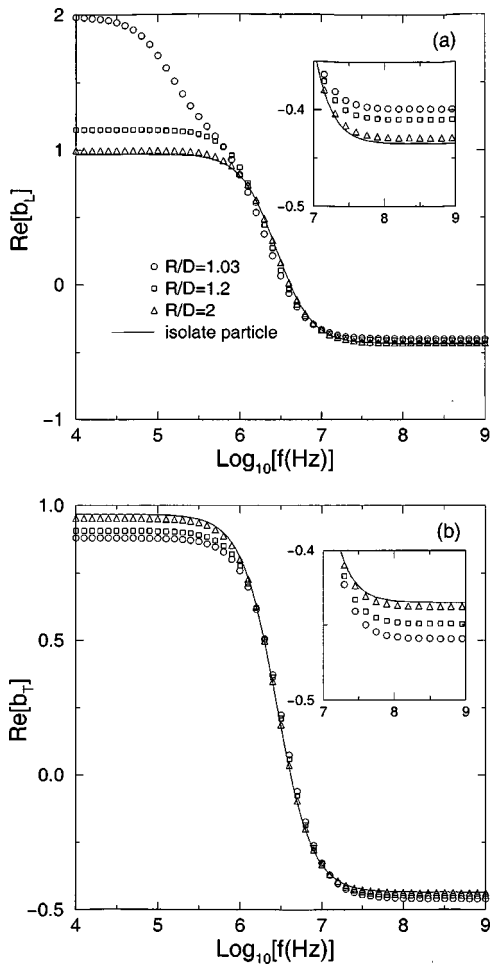


FIG. 4. Similar to Fig. 1 but for three different reduced separations  $R/D$ . Insets: Enlargement of the high frequency spectrum for clarity. Parameters:  $s = 1.1$ ,  $t = -1/90$  and  $\sigma_2 = 2.8 \times 10^{-4}$  S/m.

lected small variation of  $s$  because the variation of real dielectric constants of various typical colloidal particles is small indeed. This figure shows that  $s$  has essentially no effect on the DEP force at low frequencies, but a minor effect at high frequencies. In addition, unlike the  $t$  effect (Fig. 1),

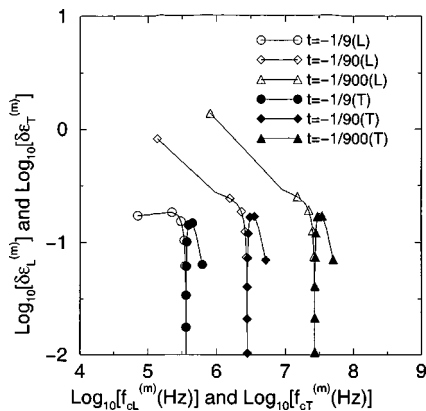


FIG. 5. The dispersion magnitude  $\delta\epsilon^{(m)}$  vs the characteristic frequency  $f_c^{(m)}$  for two touching spheres at various  $R/D$ 's for the longitudinal (open symbols) and transverse (filled symbols) cases. The lines are guides to the eyes.

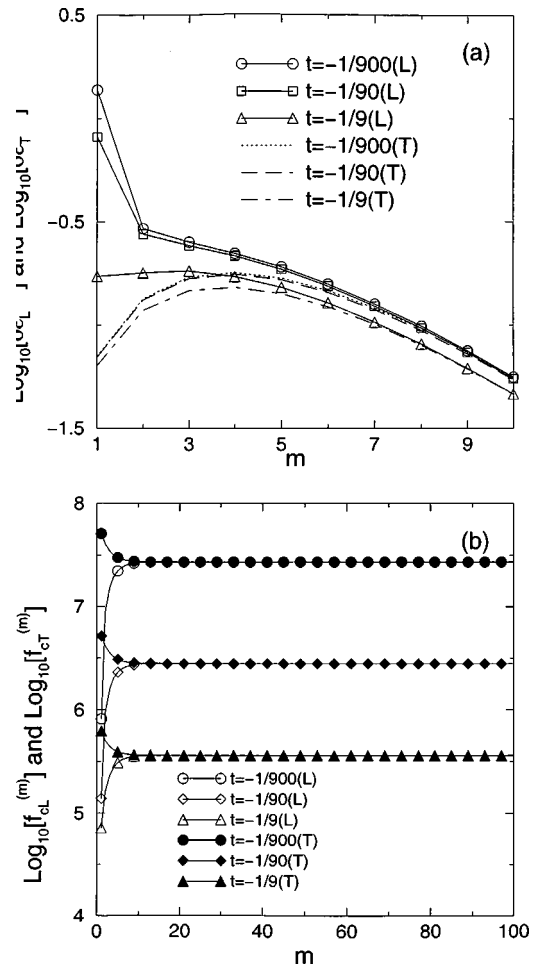


FIG. 6. The dispersion magnitude  $\delta\epsilon^{(m)}$  and the characteristic frequency  $f_c^{(m)}$  plotted vs  $m$  for two touching spheres at various  $t$  for the longitudinal ( $L$ ) and transverse ( $T$ ) cases.

the parameter  $s$  variation does not change the location of the dispersions or the crossover frequency.

The effect of medium conductivity  $\sigma_2$  on the DEP spectrum is shown in Fig. 3. Obviously, decreasing  $\sigma_2$  leads both the dispersions and the crossover frequencies to move to lower frequencies (redshifted) either in touching case (symbols) or isolated case (lines).

The dependence of the DEP force on the separations between particles is shown in Fig. 4, in an attempt to discuss the effect of multiple images. It is found that the effect of multiple images is small enough to be neglected, especially at large separations (such as,  $R/D \geq 2.0$ ), as expected. In other words, the multiple images play an important role in the case where the particles are close enough. Actually, this result is quite reminiscent of that in a recent work<sup>16</sup> where we discussed the electrorotation spectrum of a pair of touching particles.

In Fig. 5, we plot the dispersion magnitude ( $\delta\epsilon_L^{(m)}$  and  $\delta\epsilon_T^{(m)}$ ) versus the characteristic frequencies ( $f_{cL}^{(m)}$  and  $f_{cT}^{(m)}$ ), for  $m = 1 - 100$  with different medium conductivity  $\sigma_2$ . Here  $\delta\epsilon^{(m)}$  and  $f_c^{(m)}$  are the  $m$ th dispersion strength and characteristic frequency, respectively. As shown in Sec. II A, an infinite number of subdispersions exist, but most of them are located close to the main dispersion, and converge to the

main dispersion ( $m \geq 5$ ) as  $m$  increases, both for the longitudinal field and transverse field cases. This is the reason why only one or two dispersions are visible in Figs. 1–4.

For a better understanding of the  $m$  dependence of  $m$ th dispersion strength and characteristic frequency, we plot the dispersion magnitudes ( $\delta\epsilon_L^{(m)}$  and  $\delta\epsilon_T^{(m)}$ ) as a function of  $m$  [Fig. 6(a)], and the characteristic frequencies ( $f_{cL}^{(m)}$  and  $f_{cT}^{(m)}$ ) [Fig. 6(b)].

Figures 5 and 6 show that the difference between the longitudinal field and transverse field cases is quite large, especially at small  $m$ ; however, at large  $m$ , this difference disappears. From the analysis of the spectral representation theory (see Fig. 5 or Fig. 6), we can conclude that the appearance of the one subdispersion in Figs. 1–4 is actually due to the overlap of the infinite subdispersions. In a word, by using the spectral representation theory in Fig. 5 (or Fig. 6), we can understand our results more clearly.

#### IV. DISCUSSION AND CONCLUSION

Here some comments are in order. In view of the results of a two-particle system under consideration in the present work, an extension to the high concentration case is necessary. In doing so, we could resort to an effective medium theory to include the many-body (local-field) effect.<sup>19</sup>

The present theory can be applied to investigate the dependence of DEP spectra on gradation (inhomogeneity)<sup>20,21</sup> inside colloidal particles or biological cells.

To sum up, we discussed the DEP spectrum of a pair of touching polarizable colloidal particles. For two touching particles, the multiple images effect plays an important role in their respective dipole moment and the DEP spectrum, especially at low frequencies. Our methods was based on the multiple image method. We found the multiple images have a crucial effect on the DEP spectrum, but a weak effect on the crossover frequency. Our results can be well understood

by using the spectral representation theory. As a result, the present results will show some clues on the correlation effect between the colloidal particles in ac electrokinetic phenomena.

#### ACKNOWLEDGMENTS

This work has been supported by the Research Grants Council of the Hong Kong SAR Government under Project Nos. CUHK 4245/01P and CUHK 403303.

- <sup>1</sup>H. A. Pohl, *Dielectrophoresis* (Cambridge University Press, Cambridge, 1978).
- <sup>2</sup>M. P. Hughes, H. Morgan, F. J. Rixon, J. P. H. Burt, and R. Pethig, *Biochim. Biophys. Acta* **1425**, 119 (1998).
- <sup>3</sup>H. Morgan, M. P. Hughes, and N. G. Green, *Biophys. J.* **77**, 516 (1999).
- <sup>4</sup>J. P. Huang, M. Karttunen, K. W. Yu, and L. Dong, *Phys. Rev. E* **67**, 021403 (2003).
- <sup>5</sup>X. Duan, Y. Huang, Y. Cui, J. Wang, and C. M. Lieber, *Nature (London)* **409**, 66 (2001).
- <sup>6</sup>C. Marquet, A. Buguin, L. Talini, and P. Silberzan, *Phys. Rev. Lett.* **88**, 168301 (2002).
- <sup>7</sup>C. F. Chou, J. O. Tegenfeldt, O. Bakajin, S. S. Chan, E. C. Cox, N. Darnton, T. Duke, and R. H. Austin, *Biophys. J.* **83**, 2170 (2002).
- <sup>8</sup>K. Ratanachoo, P. R. C. Gascoyne, and M. Ruchirawat, *Biochim. Biophys. Acta* **1564**, 449 (2002).
- <sup>9</sup>Y. Huang, S. Joo, M. Duhon, M. Heller, B. Wallace, and X. Xu, *Anal. Chem.* **74**, 3362 (2002).
- <sup>10</sup>T. B. Jones and T. N. Tombs, *Inst. Phys. Conf. Ser.* **118**, 39 (1991).
- <sup>11</sup>K. W. Yu and Jones T. K. Wan, *Comput. Phys. Commun.* **129**, 177 (2000).
- <sup>12</sup>H. Sun and K. W. Yu, *Phys. Rev. E* **67**, 011506 (2003).
- <sup>13</sup>H. J. H. Clercx and G. Bossis, *Phys. Rev. E* **48**, 2721 (1993).
- <sup>14</sup>D. J. Bergman, *Phys. Rep.* **43**, 377 (1978).
- <sup>15</sup>T. B. Jones, *Electromechanics of Particles* (Cambridge University Press, New York, 1995).
- <sup>16</sup>J. P. Huang, K. W. Yu, and G. Q. Gu, *Phys. Rev. E* **65**, 021401 (2002).
- <sup>17</sup>T. B. Jones, *J. Electrostat.* **25**, 231 (1990).
- <sup>18</sup>J. Lei, Jones T. K. Wan, K. W. Yu, and H. Sun, *Phys. Rev. E* **64**, 012903 (2001).
- <sup>19</sup>L. Gao, J. P. Huang, and K. W. Yu, *Phys. Rev. E* **67**, 021910 (2003).
- <sup>20</sup>J. P. Huang, K. W. Yu, G. Q. Gu, and M. Karttunen, *Phys. Rev. E* **67**, 051405 (2003).
- <sup>21</sup>L. Dong, G. Q. Gu, and K. W. Yu, *Phys. Rev. B* **67**, 224205 (2003).